SLAC-PUB-4393
DPNU-87-45
September 1987
(M)

OBSERVATION OF THE SELECTIVE COUPLING OF K^* STATES TO THE $K^-\eta$ CHANNEL*

D. ASTON,[1] N. AWAJI,[2a] T. BIENZ,[1] F. BIRD,[1] J. D'AMORE,[3]
W. DUNWOODIE,[1] R. ENDORF,[3] K. FUJII,[2b] H. HAYASHII,[2c] S. IWATA,[2b]
W.B. JOHNSON,[1] R. KAJIKAWA,[2] P. KUNZ,[1] D.W.G.S. LEITH,[1] L. LEVINSON,[1d]
T. MATSUI,[2b] B.T. MEADOWS,[3] A. MIYAMOTO,[2b] M. NUSSBAUM,[3] H. OZAKI,[2]
C.O. PAK,[2b] B.N. RATCLIFF,[1] D. SCHULTZ,[1] S. SHAPIRO,[1] T. SHIMOMURA,[2e]
P. K. SINERVO,[1f] A. SUGIYAMA,[2] S. SUZUKI,[2] G. TARNOPOLSKY,[1g]
T. TAUCHI,[2b] N. TOGE,[1] K. UKAI,[4] A. WAITE,[1h] S. WILLIAMS[1i]

[1]*Stanford Linear Accelerator Center, Stanford University, P.O. Box 4349, Stanford, California 94305, U.S.A.*
[2]*Department of Physics, Nagoya University, Furo-cho, Chikusa-ku, Nagoya 464, Japan*
[3]*University of Cincinnati, Cincinnati, Ohio 45221, U.S.A.*
[4]*Institute for Nuclear Study, University of Tokyo, Midori-cho, Tanashi, Tokyo 188, Japan*

ABSTRACT

The $K^-\eta$ effective mass spectrum in the reaction $K^-p \to K^-\pi^+\pi^-\pi^0 p$ at 11 GeV/c has a prominent peak at $\sim$ 1.75 GeV/c^2, which is shown to be due to the $K_3^*(1780)$ by a spherical harmonic moments analysis and amplitude decomposition; there is no significant signal for $K_2^*(1430)$. The measured branching fractions for the leading $L = 1$ and $L = 2$ K^*'s, $[BF(K_2^*(1430) \to K\eta) < 0.45\%$ at the 95% c.l., and $BF(K_3^*(1780) \to K\eta) = 9.4 \pm 3.4$ %] confirm the SU(3) prediction that the $K\eta$ channel couples preferentially to odd spin K^*'s.

Submitted to *Phys. Letters B*

---

* Work supported in part by the Department of Energy under contract No. DE-AC03-76SF00515; the National Science Foundation under grant Nos. PHY82-09144, PHY85-13808, and the Japan U.S. Cooperative Research Project on High Energy Physics.

Present Addresses :

a Fujitsu Limited, Nakahara-ku, Kawasaki 211, Japan.
b National Laboratory for High Energy Physics, KEK, Oho-machi, Tsukuba, Ibaraki 305, Japan.
c Nara Women's University, Kitauoya-nishi-machi, Nara-shi, Nara 630, Japan.
d Weizmann Institute, Rehovot 76100, Israel.
e Nippon BIO-RAD Laboratories, 1-2-7 Shiba-Daimon, Minato-ku, Tokyo 105, Japan.
f University of Pennsylvania, Philadelphia, Pennsylvania 19104, U.S.A.
g Hewlett-Packard Laboratories, 1501 Page Mill Road, Palo Alto, California 94304, U.S.A.
h Department of Physics, University of Victoria, Victoria BC, Canada V8W 2Y2
i Diasonics Corp., 533 Cabot Rd., S. San Francisco, CA 94090, U.S.A.

There have been extensive studies of the strange mesons (K^*) in the $K\pi$ and $K\pi\pi$ final states [1,2,3,4,5], and the decay branching fractions (BF) of the leading and underlying states below 2.0 GeV/c^2 to these channels are relatively well measured. However, no significant direct observation of K^* decay to the $K\eta$ final state has been reported so far [6]; the PDG summary table [7] cites only an indirect measurement of the $BF(K_2^*(1430) \to K\eta)$ taken from a multi-channel fit.

As we discuss below, the SU(3) properties of the coupling of $K\eta$ to the K^*'s leads to the striking prediction that the $K\eta$ branching fraction for even-spin states will be extremely small, while that for odd spin states should be quite substantial. It follows that the measurement of these branching fractions provides a good check of SU(3) symmetry. The importance of measuring the $K\eta$ (and $K\eta'$) decay branching fractions and confirming the selective coupling to even and odd spin K^*'s has been pointed out by Lipkin [8], who emphasized that the same argument leads to a robust method of distinguishing between different classes of charmed meson decay models. There is some indirect evidence for the expected suppression of the $K\eta$ decay mode for the spin zero K^*, since the S-wave $K\pi$ amplitude is fully elastic well above the $K\eta$ threshold [4], but direct confirmation for other K^* states has not been made until now because of experimental limitations.

In this paper, we present an analysis of the $K^-\eta$ system produced in the reaction

$$K^-p \to K^-\pi^+\pi^-\pi^0 p \tag{1}$$

at 11 GeV/c. The data were obtained with the Large Aperture Superconducting Solenoid (LASS) spectrometer at SLAC. The LASS spectrometer is characterized by a clean RF separated K^- beam, flat acceptance over nearly 4π steradians, and a bias-free trigger for events with $\geq$2 charged particles. It consists of a solenoidal vertex detector, a downstream dipole spectrometer and particle identification devices. Cylindrical and

planar proportional chambers surround the hydrogen target to detect particles with $\sim 4\pi$ solid angle in the magnetic field of 22.4 kG provided by the superconducting solenoid. High momentum, forward going particles are measured by the dipole spectrometer. Good particle identification is provided by two threshold Čerenkov counters located at the end of solenoid and dipole spectrometers with a π threshold at 2.6 GeV/c and 2.9 GeV/c respectively, a time of flight counter hodoscope downstream of the solenoid, and dE/dx measurement in the cylindrical proportional chamber package around the target. The details of the spectrometer are described elsewhere [9]. The sensitivity of the experiment is 4.1 events/nb, and the resulting $K^-\eta$ sample is at least twenty times larger than that obtained in any other experiment [6].

Four-prong events with net charge zero are selected as candidates for reaction (1), and the following rather loose kinematical requirements are imposed: (a) for at least one mass assignment permutation, the missing mass squared (MM^2) recoiling against $K^-\pi^+\pi^-p$ must satisfy $|MM^2| < 0.3$ (GeV/c^2)^2; (b) the four momentum transfer squared, $t' = |t_{p\to p}| - |t_{p\to p}|_{min}$, must satisfy $t' \leq 2.0$ (GeV/c)^2 for at least one of the accepted mass permutations; and (c) with the assumption that the missing momentum vector corresponds to a π^0, the effective mass of the three pion system for at least one of the surviving mass permutations must satisfy $M_{\pi^+\pi^-\pi^0} \leq 1.1$ GeV/c^2. The remaining events are refit with full kinematic constraints to the track coordinates to distinguish reaction (1) from the predominant diffractive background process $K^-p \to K^-\pi^+\pi^-p$; events are removed if they satisfy this hypothesis with confidence level $\geq 10^{-10}$ for at least one possible particle assignment. Next, a fit to reaction (1) is performed, and events are accepted if the fit has a confidence level $\geq 10^{-2}$. Čerenkov counter information is then used to separate K's from π's above 3.0 GeV/c, and TOF information to separate π's from p's below 2.3 GeV/c. Finally, to reduce the remaining background, the $MM^2(K^-\pi^+\pi^-p)$ is required to be between -0.15 and 0.1 (GeV/c)^2. This results in a unique assignment of the charged particle masses for 87.7% of the

events. A two-fold ambiguity remains for 11.9% of the sample, and the remaining 0.4% have more ambiguities. The remaining ambiguities are resolved by choosing the particle assignment that gives the largest confidence level fit.

Fig. 1

The $\pi^+\pi^-\pi^0$ mass spectrum shows clear η and ω signals (fig. 1a) which are well-described by Gaussians centered at mass values $M_\eta = 548.0 \pm 0.4$ MeV/c^2 and $M_\omega = 782.6 \pm 0.1$ MeV/c^2, in excellent agreement with the PDG values [7]; the corresponding values of σ, $\sigma_\eta = 9.7$ MeV/c^2 and $\sigma_\omega = 19.2$ MeV/c^2, are consistent with the expected mass resolution.

Selecting the η mass region (0.52 - 0.57 GeV/c^2), which contains 7626 events with a signal-to-noise ratio of about one (fig. 1b), the $K^-\eta$ effective mass spectrum of fig. 2a shows a prominent peak at ~1.75 GeV/c^2 and no other significant structure. In particular, there is no structure in the region of the $K_2^*(1430)$. The Dalitz plot (not shown) demonstrates that the high mass region contains the reflection of substantial low mass N^* and Y^* production. These backgrounds are removed by requiring $M_{\eta p}$ >2.00 GeV/c^2 and M_{K^-p} >1.85 GeV/c^2, resulting in the hatched histogram of fig. 2a.

Fig. 2

The acceptance-corrected spherical harmonic moments ($t_{lm} = \sqrt{4\pi} N < Y_{lm} >$) in the t channel helicity frame are obtained by the moments method for $0.08 \leq t' < 1.0$ (GeV/c)^2. The cut at low t' is necessary since recoil protons of momentum $\leq$ 270 MeV/c do not escape from the target volume. A substantial portion of the data in the selected sample comes from the non-η background below the η peak. For each moment, this background is estimated in 100 MeV/c^2 bins (two adjacent bins combined) of $K^-\pi^+\pi^-\pi^0$ mass by fitting the $\pi^+\pi^-\pi^0$ mass spectrum, with each event weighted by its value of the spherical harmonic function in question, to a Gaussian resolution function for the η signal plus a second order polynomial for the background. The background moments are smooth in mass, and only moments with small l are significant. The resulting background-subtracted acceptance-corrected $K\eta$ mass spectrum (i.e. t_{00}) is

displayed in fig. 2b, and the corresponding moments with $l \geq 1$ are shown in fig. 3. There is clear structure in the region around 1.75 GeV/c^2 in moments with $l \leq 6$. Since moments with $l > 6$ are not significant, this structure is indicative of the presence of a spin 3 resonance near 1.75 GeV/c^2. There is no evidence of significant structure elsewhere.

Fig. 3

The spherical harmonic moments can be expressed as bilinear products of production amplitudes $L_{\lambda\pm}$ of the $K^-\eta$ system with spin L and t-channel helicity λ, via natural (+) or unnatural (−) parity exchange [10]. Since moments with $m > 2$ are not required, the amplitudes with $\lambda > 1$ can be neglected and all moments up to $l = 6$, $m = 2$ used to determine the amplitudes S_0, P_0, $P_\pm$, D_0, $D_\pm$, F_0 and $F_\pm$, where we have adopted the simplified notation, $L_0 \equiv L_{0-}$, and $L_\pm \equiv L_{1\pm}$. In the summed intensities of fig. 4, only the F wave has significant peak structure. There are ambiguities in the region above 1.5 GeV/c^2, but, in general, the other solutions agree with the one shown within the statistical errors. A fit to $|F|^2_{tot}$ with a relativistic Breit-Wigner form gives $M = 1749 \pm 10$ MeV/c^2 and $\Gamma = 193^{+51}_{-37}$ MeV/c^2 ($\chi^2/N_{DF} = 7.0/8$), where the quoted errors are statistical only. The systematic error on the mass, estimated by using different N^* cuts, is approximately as large as the statistical error.

Fig. 4

Given the results of the moment analysis and the amplitude decomposition, the peak around 1.75 GeV/c^2 is most naturally interpreted as the $J^P = 3^-$ $K_3^*(1780)$.

Fig. 5 shows the detailed decomposition of the F wave amplitude. Both $|F_0|^2$ and $|F_+|^2$ show strong peaks at the $K_3^*(1780)$, while there is no contribution from $|F_-|^2$ (figs. 5a-c). The t' dependences of the significant amplitudes, $|F_0|^2$ and $|F_+|^2$, in the $K_3^*(1780)$ region (1.60 − 1.95 GeV/c^2) are shown in figs. 5d and 5e. These distributions are fit by the forms $A_0 \frac{-t}{(m_\pi^2 - t)^2} e^{-B_0 t'}$ for $|F_0|^2$, and $A_+ \; t' \; e^{-B_+ t'}$ for $|F_+|^2$ in the t' region $0.08 \leq t' < 1.00$ (GeV/c)^2, yielding slope parameter values $B_0 = 5.9 \pm 1.4$ (GeV/c)$^{-2}$ and $B_+ = 9.2 \pm 0.8$ (GeV/c)$^{-2}$. Integrating the Breit-Wigner

formulae for the $|F_0|^2$ and $|F_+|^2$ over the mass region $1.4 - 2.2$ GeV/c^2, and correcting for the $\eta \to \pi^+\pi^-\pi^0$ decay branching fraction, the $K\eta$ channel cross section in the measured t' region (0.08-1.0 (GeV/c)^2) is found to be 2.30 ± 0.23 μb. After correcting for the t' region below 0.08 (GeV/c)^2 using the fitted expressions above, the cross section times branching fraction in the full t' region is estimated to be $\sigma(K_3^{*-}(1780)) \cdot BF(K_3^{*-}(1780) \to K^-\eta) = 3.90 \pm 0.55$ μb (systematic error included). The error comes mainly from the extrapolation of the t' distribution to $t' = 0$. Taking the cross section $\sigma(K_3^{*-}(1780)) \cdot BF(K_3^{*-}(1780) \to K\pi) = 7.8 \pm 2.6$ μb from the interpolation formula given by the CERN-Geneva group [5], the $K\eta$ to $K\pi$ branching ratio is

$$R_3 = \frac{\Gamma(K_3^*(1780) \to K\eta)}{\Gamma(K_3^*(1780) \to K\pi)} = 0.50 \pm 0.18.$$

We note that the precision of this measurement will be significantly improved in the near future by using high statistics data on K^{*-} production in the reaction $K^-p \to K_s^0\pi^-p$ from the present experiment [11]. Taking the most precise measured value for the $BF(K^*(1780) \to K\pi)$, viz. $18.7 \pm 1.2\%$ [3], we obtain $BF(K_3^*(1780) \to K\eta) = 9.4 \pm 3.4\%$.

Fig. 5

In contrast, there is no evidence for the production of $K_2^*(1430)$ in either the $K^-\eta$ mass spectrum (fig. 2) or the D-wave intensity distribution (fig. 4), even though the $K_2^*(1430)$ production cross section is known to be large [5]. Taking the production cross section for the $K_2^*(1430)$ into $K\pi$ from ref. 5, the upper limit on the $K\eta$ to $K\pi$ branching ratio is estimated from $|D|^2_{tot}$ to be

$$R_2 = \frac{\Gamma(K_2^*(1430) \to K\eta)}{\Gamma(K_2^*(1430) \to K\pi)} < 0.0092$$

at the 95% confidence level. Using the value $BF(K_2^*(1430) \to K\pi) = 48.5\%$ [3], we find an upper limit for $BF(K_2^*(1430) \to K\eta)$ of 0.45% at the 95% confidence level. This is substantially smaller than the value 5.2 ± 2.9 % which is obtained indirectly by the Particle Data Group from a multi-channel fit [7].

The dramatic difference between the $K\eta$ coupling to the $K_2^*(1430)$ and the $K_3^*(1780)$ can be explained in an SU(3) model with octet-singlet mixing of η and η' [8]. The SU(3) $K^*\overline{K}\eta$ three meson couplings are either F or D type according to the symmetry of parent and daughter meson states. A straight-forward calculation gives

$$R_2 = \frac{\Gamma(K_2^*(1430) \to K\eta)}{\Gamma(K_2^*(1430) \to K\pi)} = \frac{1}{9}(cos\theta_p + 2\sqrt{2}sin\theta_p)^2 \left(\frac{q_{K\eta}}{q_{K\pi}}\right)^5$$

and

$$R_3 = \frac{\Gamma(K_3^*(1780) \to K\eta)}{\Gamma(K_3^*(1780) \to K\pi)} = (cos\theta_p)^2 \left(\frac{q_{K\eta}}{q_{K\pi}}\right)^7$$

where $q_{K\eta}$ ($q_{K\pi}$) is the kaon momentum in the $K\eta$ ($K\pi$) rest frame, and θ_p is the SU(3) singlet-octet mixing angle for the pseudoscalar nonet. Since θ_p is known to be negative and $\sim -20°$, R_2 suffers a significant suppression over and above that resulting from the explicit factor of 9, due to the expression in parentheses. On the other hand, R_3 is rather insensitive to θ_p. For example, the branching ratios are as follows for representative values of θ_p :

$\theta_p = -10.0° : R_2 = 0.008, R_3 = 0.41$ (quadratic mass formula) ;

$\theta_p = -19.5° : R_2 = 0.000, R_3 = 0.38$;

$\theta_p = -23.0° : R_2 = 0.001, R_3 = 0.36$ (linear mass formula) .

The measured value of R_3 and the upper limit on R_2 are consistent with all of the above predicted values. In this regard we note that a recent review by Gilman and Kauffman [12] concludes that $\theta_p \sim -20°$ is consistent with all of the relevant physical evidence.

In SU(3), the features described above apply to all K^* states in that $K\eta$ couples preferentially to odd spin K^*'s, and almost not at all to even spin K^*'s. For the $K\eta'$ channel the situation is reversed; even spin K^*'s are expected to couple preferentially to $K\eta'$, while decay modes such as $K_3^*(1780) \to K\eta'$ are expected to be suppressed.

Further exploration of the underlying K^* states in the $K\eta$ channel, and studies of $K^* \to K\eta'$ decay modes would be necessary to reinforce these conclusions.

In summary, we have made a clear observation of the $K^-\eta$ decay of the $K_3^*(1780)$ and have established an upper limit for the $K\eta$ decay of the $K_2^*(1430)$ which is significantly lower than the value quoted by the Particle Data Group [7]. The $BF(K_3^*(1780) \to K\eta)$ is measured to be 9.4 ± 3.4 %, while the $BF(K_2^*(1430) \to K\eta)$ is shown to be less than 0.45% at the 95% confidence level. These results provide clear experimental evidence for the suppression of the $K_2^*(1430)$ coupling to $K\eta$, and for the relatively large coupling of the $K_3^*(1780)$ to this channel predicted from SU(3) with octet-singlet mixing of η-η'.

The authors are grateful to Profs. H. J. Lipkin and J. Rosner for stimulating discussions, and are indebted to the technical staffs of SLAC, Group B, and the High Energy Physics Laboratory at Nagoya University.

REFERENCES

1. D. Aston et al., Phys. Lett. 99B (1981) 502
   D. Aston et al., Phys. Lett. 106B (1981) 235
   D. Aston et al., Phys. Lett. 149B (1984) 258
   D. Aston et al., Nucl. Phys. B247 (1984) 261
   D. Aston et al., Phys. Letters 180B (1986) 308
2. C. Daum et al., Nucl. Phys. B187 (1981) 1
3. D. Aston et al., SLAC-PUB-4260/DPNU-87-25 ,
   to be published in Nucl. Phys. B
4. P. Estabrooks et al., Nucl. Phys. B133 (1978) 490
   P. Estabrooks, Phys. Rev. D19 (1979) 2678
5. W. E. Cleland et al., Nucl. Phys. B208 (1982) 189
   A. D. Martin et al., Nucl. Phys. B134 (1978) 392
6. J. Badier et al., Phys. Letters 19 (1965) 612
   G. Bassompiere et al., Nucl. Phys. B13 (1969) 189
   J. M. Bishop et al., Nucl. Phys. B9 (1969) 403
   M. Aguilar-Benitez et al., Phys. Rev. D4 (1971) 2583
7. Review of Particle Properties, Particle Data Group, Phys. Lett. 170B (1986) 1
8. H. J. Lipkin, Phys. Rev. Lett. 46 (1981) 1307
9. D. Aston et al., The LASS Spectrometer, SLAC-REP-298, May 1986.
10. For notation, see for example, G. Costa et al., Nucl. Phys. B175 (1980) 402
11. D. Aston et al., to be published.
12. F. J. Gilman and R. Kauffman, SLAC-PUB-4301

FIGURE CAPTIONS

1. (a) The $\pi^+\pi^-\pi^0$ effective mass distribution for the mass region below 1.0 GeV/c^2; (b) an expanded plot in the vicinity of the η ; the hatched area indicates the η region used in the analysis.

2. (a) The $K^-\pi^+\pi^-\pi^0$ effective mass distribution for the η region used in the analysis ; the hatched histogram shows the result of requiring $M_{\eta p} > 2.00$ GeV/c^2 and $M_{K^-p} > 1.85$ GeV/c^2;
   (b) the background-subtracted and acceptance-corrected $K^-\eta$ mass spectrum (the t_{00} moment).

3. The acceptance-corrected spherical harmonic moments , t_{lm} , with $l \geq 1$ and $m \leq 2$.

4. The intensity distribution for each spin state, where $|L|^2_{tot} = |L_0|^2 + |L_-|^2 + |L_+|^2$; the curve superposed on $|F|^2_{tot}$ shows the result of the Breit-Wigner fit described in the text, while that on the $|D|^2_{tot}$ intensity shows the 95 % confidence level upper limit for $K^*_2(1430)$ production.

5. (a)- (c) The mass dependence of the F-wave intensity contributions; the curves on $|F_0|^2$ and $|F_+|^2$ are the results of the Breit-Wigner fits described in the text; (d),(e) the t' dependence of $|F_0|^2$ and $|F_+|^2$, respectively, in the $K^*_3(1780)$ region (1.60 - 1.95 GeV/c^2); the curves show the results of the fits described in the text.

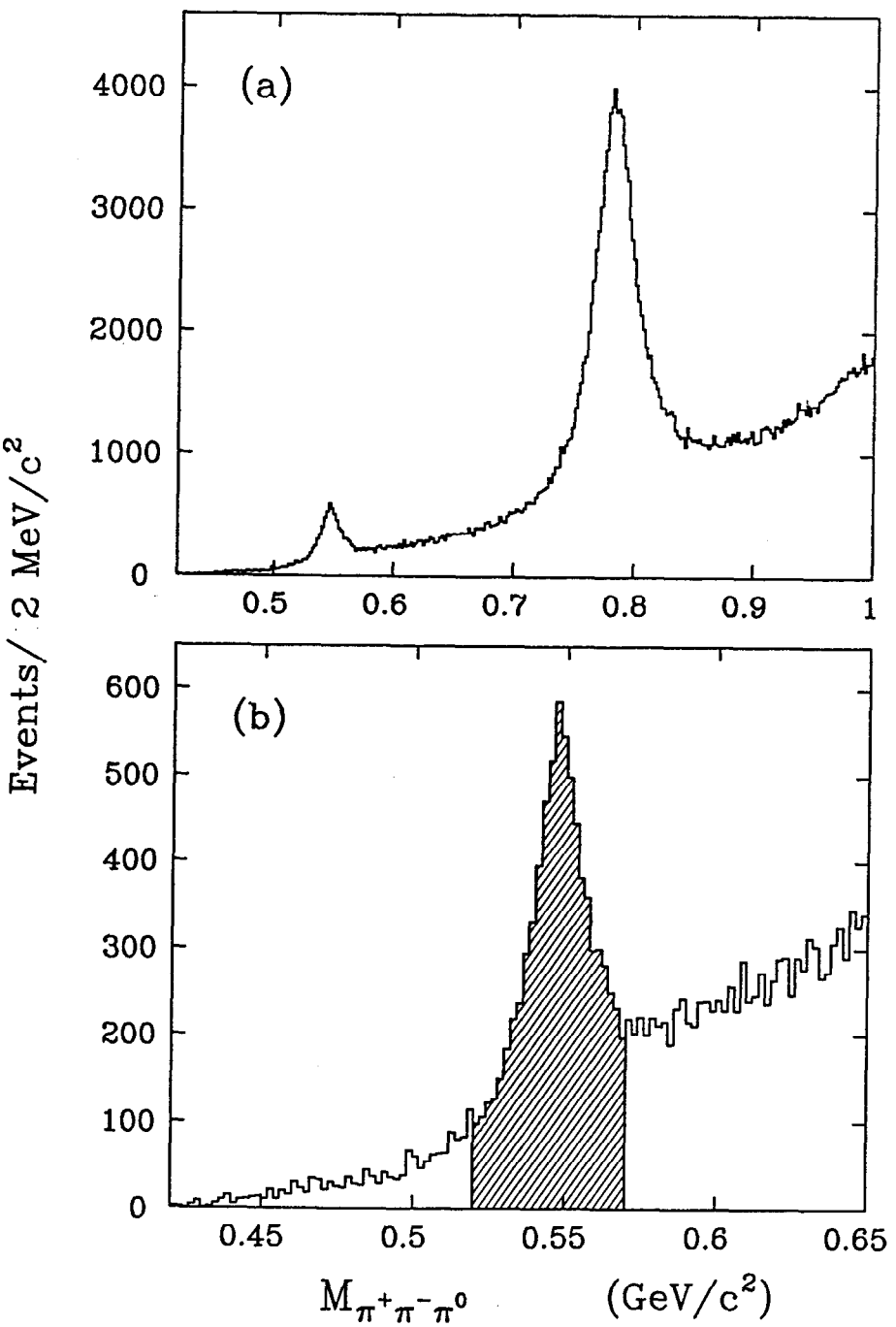
(a)
4000
3000
2000
1000
0
0.5
0.6
0.7
0.8
0.9
1
(b)
600
500
400
300
200
100
0
0.45
0.5
0.55
0.6
0.65
Events/ 2 MeV/c^2
$M_{\pi^+\pi^-\pi^0}$ (GeV/c^2)

Fig. 1

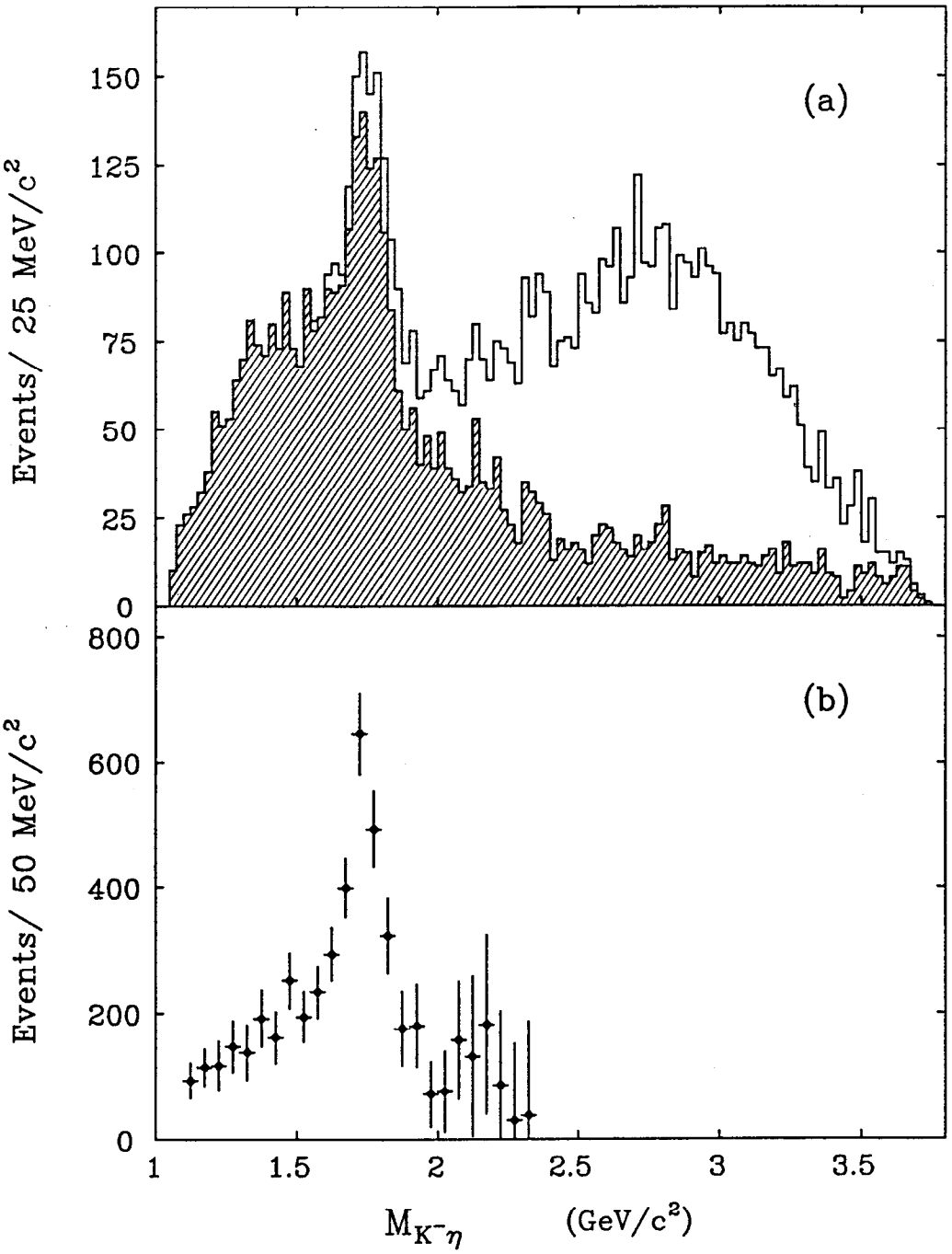
(a)
(b)
Events/ 25 MeV/c²
Events/ 50 MeV/c²
150
125
100
75
50
25
0
800
600
400
200
0
1
1.5
2
2.5
3
3.5
M K⁻η (GeV/c²)

Fig. 2

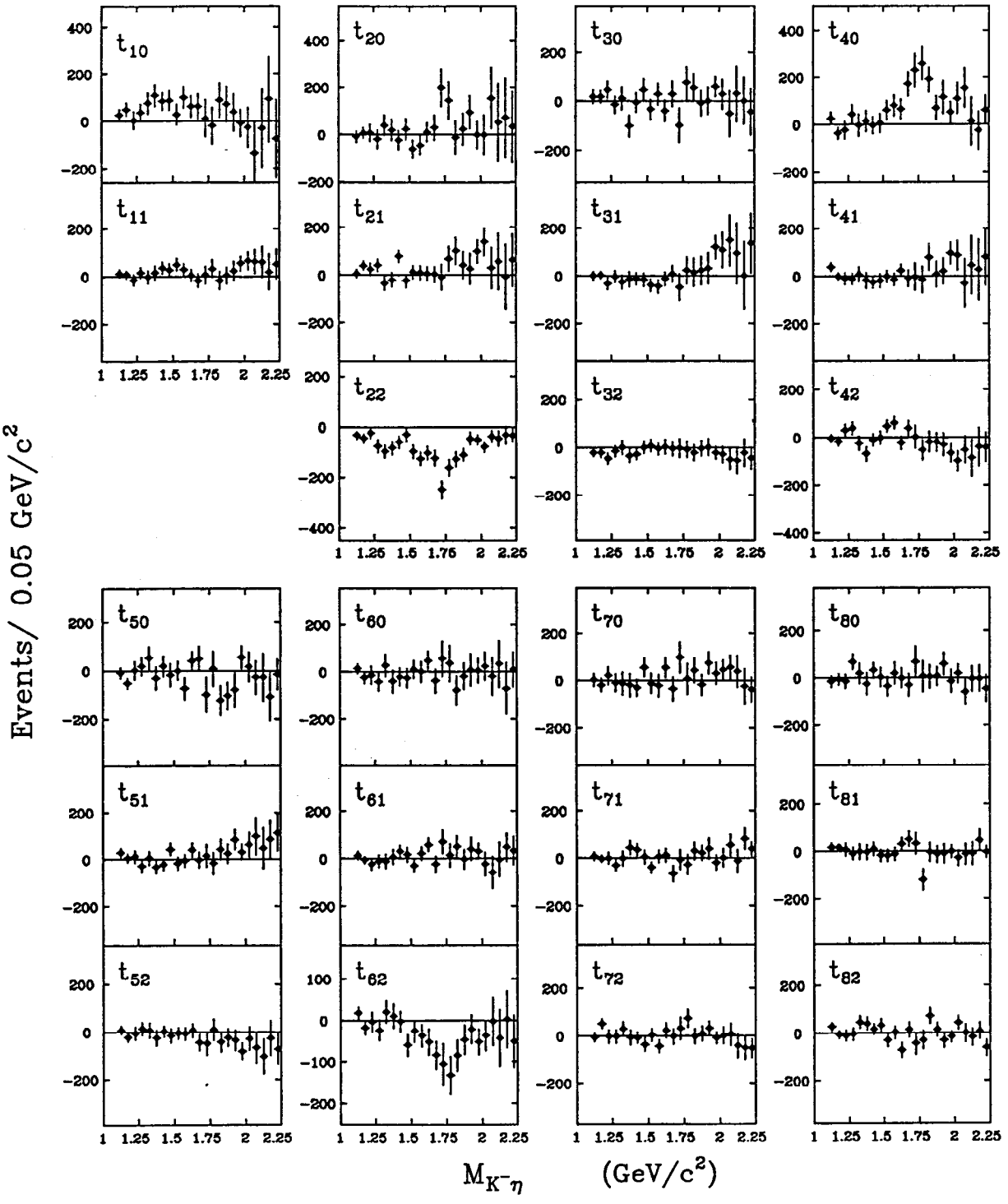
Events/ 0.05 GeV/c^2
t_{10}
t_{11}
t_{20}
t_{21}
t_{22}
t_{30}
t_{31}
t_{32}
t_{40}
t_{41}
t_{42}
t_{50}
t_{51}
t_{52}
t_{60}
t_{61}
t_{62}
t_{70}
t_{71}
t_{72}
t_{80}
t_{81}
t_{82}
$M_{K^-\eta}$ (GeV/c^2)

Fig.3

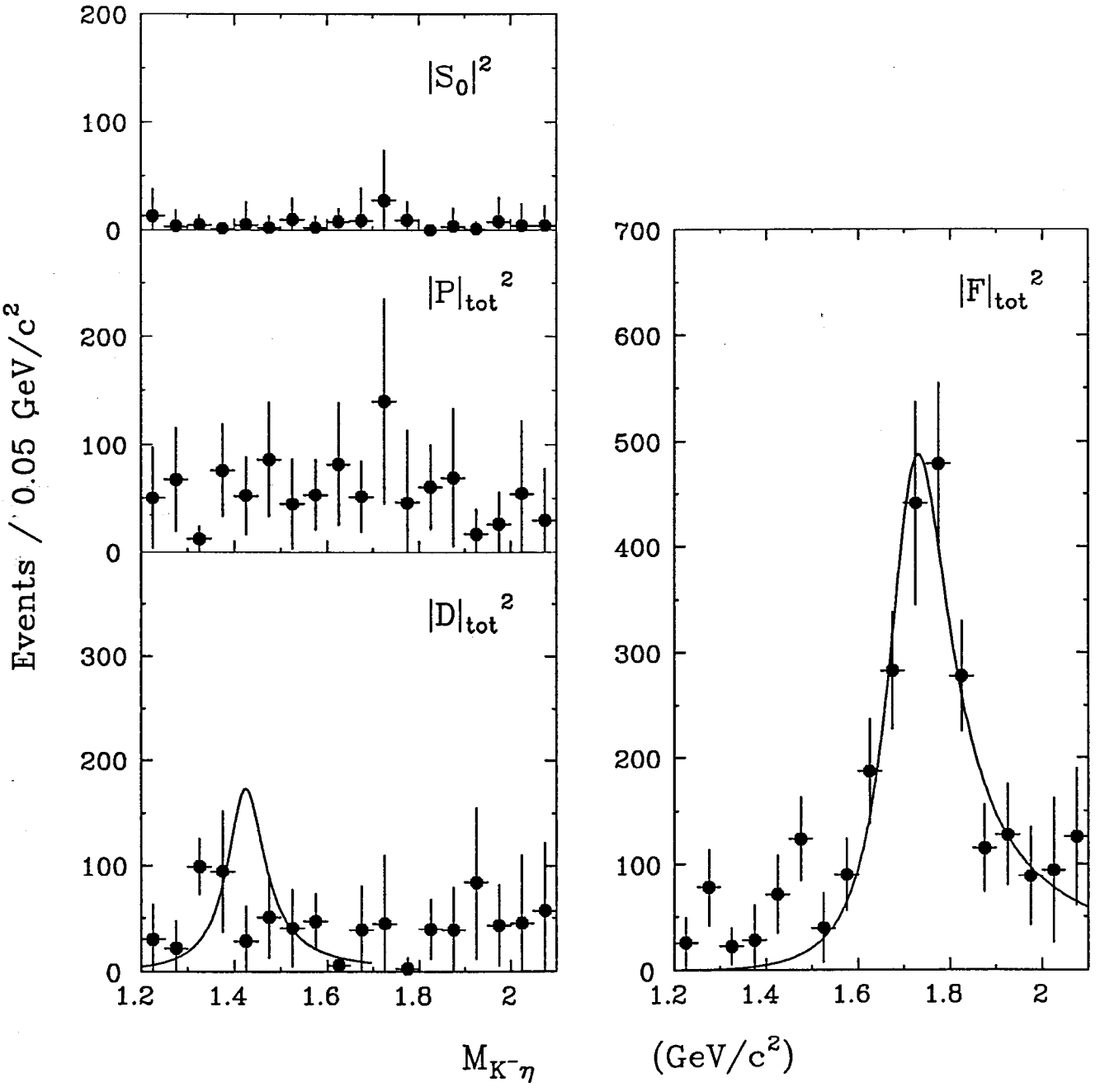
Events / 0.05 GeV/c²
|S0|²
|P|tot²
|D|tot²
|F|tot²
200
100
0
200
100
0
300
200
100
0
700
600
500
400
300
200
100
0
1.2
1.4
1.6
1.8
2
MK⁻η
(GeV/c²)

Fig. 4

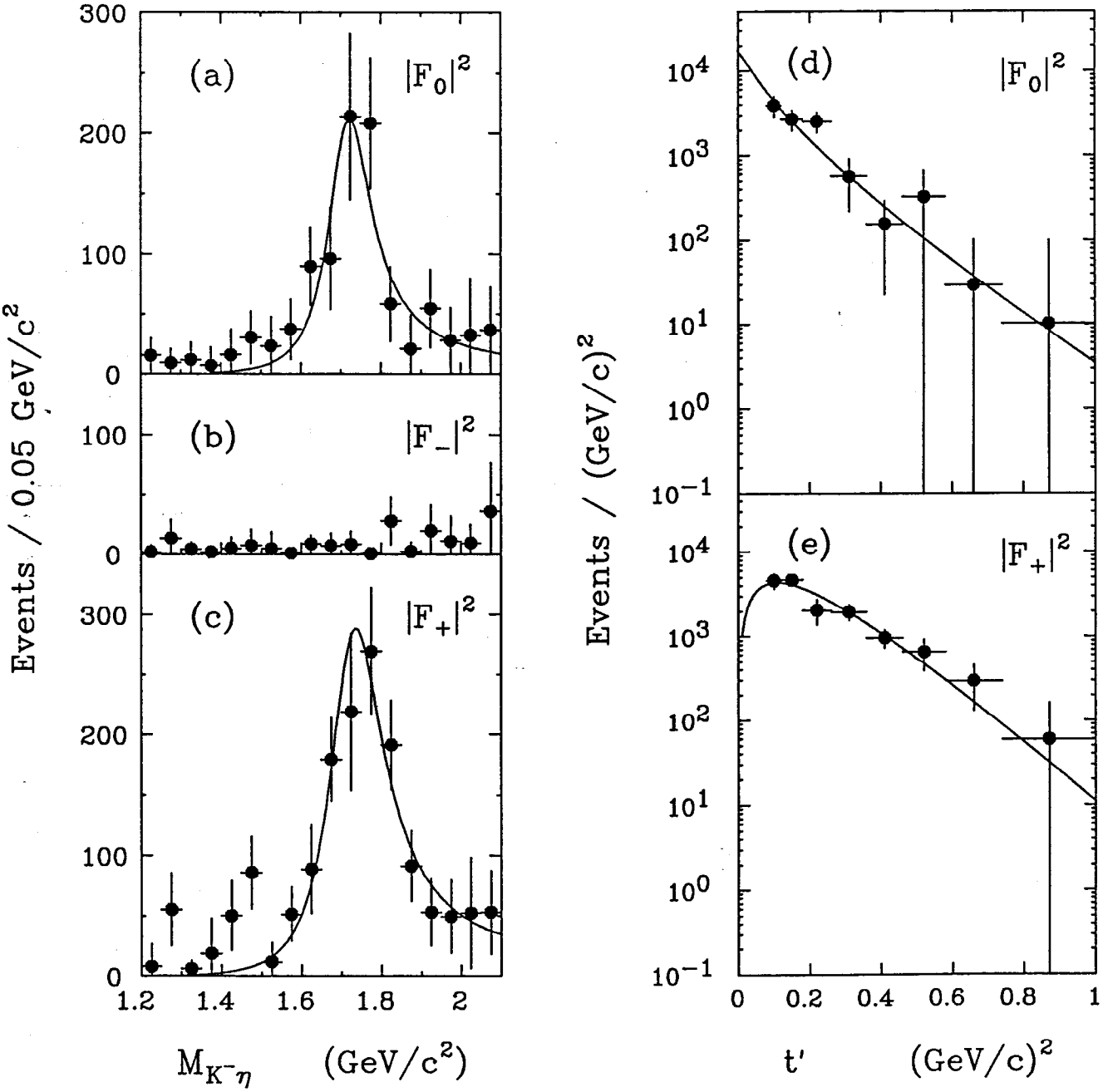
(a)
$|F_0|^2$
(b)
$|F_-|^2$
(c)
$|F_+|^2$
(d)
$|F_0|^2$
(e)
$|F_+|^2$
Events / 0.05 GeV/c^2
Events / (GeV/c)^2
$M_{K^-\eta}$ (GeV/c^2)
t' (GeV/c)^2

Fig.5